Update on electron maps for STIX

Università di Genova
DIMA | Dipartimento di Matematica

Anna Volpara, Paolo Massa, Säm Krucker,
A. Gordon Emslie, Michele Piana, Anna Maria Massone

STIX team meeting
November 07, 2023

Outline

1. From count to electron visibilities & Visibility inversion algorithm
2. Results
3. Conclusions and future works

Outline

1. **From count to electron visibilities & Visibility inversion algorithm**
2. Results
3. Conclusions and future works

From count to electron visibilities

Count visibilities:

$$V(u,v;q) = \int_X \int_Y J(x,y;q) e^{2\pi\imath(xu+yv)}\, dx\, dy \tag{1}$$

From count to electron visibilities

Count visibilities:

$$V(u,v;q) = \int_X \int_Y J(x,y;q) e^{2\pi\imath(xu+yv)}\, dx\, dy \qquad (1)$$

Count spectrum image

From count to electron visibilities

Count visibilities:

$$V(u,v;q) = \int_X \int_Y J(x,y;q) e^{2\pi\imath(xu+yv)}\, dx\, dy \qquad (1)$$

Array containing the N_V complex values of the visibilities measured by STIX

From count to electron visibilities

Count visibilities:

$$V(u,v;q) = \int_X \int_Y J(x,y;q) e^{2\pi\imath(xu+yv)}\, dx\, dy \tag{1}$$

Electron flux visibility spectrum:

$$W(u,v;E) = \int_X \int_Y \mathcal{F}(x,y;E) e^{2\pi\imath(xu+yv)}\, dx\, dy \tag{2}$$

Prato et al., *A Regularized Visibility-Based Approach to Astronomical Imaging Spectroscopy*, SIAM Journal on Imaging Sciences, (2009)

Piana et al., *Electron flux spectral imaging of solar flares through regularized analysis of hard x-ray source visibilities,* The Astrophysical Journal, (2007)

From count to electron visibilities

Count visibilities:

$$V(u,v;q) = \int_X \int_Y J(x,y;q) e^{2\pi\imath(xu+yv)}\, dx\, dy \tag{1}$$

Electron flux visibility spectrum:

$$W(u,v;E) = \int_X \int_Y \mathcal{F}(x,y;E) e^{2\pi\imath(xu+yv)}\, dx\, dy \tag{2}$$

Electron flux spectral image

$$\mathcal{F}(x,y;E) = a^2 \overline{n}_{\text{target}}(x,y)\ell(x,y)\overline{F}(x,y;E)$$

Prato et al., *A Regularized Visibility-Based Approach to Astronomical Imaging Spectroscopy*, SIAM Journal on Imaging Sciences, (2009)

Piana et al., *Electron flux spectral imaging of solar flares through regularized analysis of hard x-ray source visibilities,* The Astrophysical Journal, (2007)

From count to electron visibilities

Count visibilities:

$$V(u,v;q) = \int_X \int_Y J(x,y;q) e^{2\pi\imath(xu+yv)}\, dx\, dy \tag{1}$$

Electron flux visibility spectrum:

$$W(u,v;E) = \int_X \int_Y \mathcal{F}(x,y;E) e^{2\pi\imath(xu+yv)}\, dx\, dy \tag{2}$$

Bremsstralhung equation for visibilities:

$$V(u,v;q) = \frac{1}{4\pi R^2} \int_q^\infty W(u,v;E) K(q,E)\, dE \tag{3}$$

Prato et al., *A Regularized Visibility-Based Approach to Astronomical Imaging Spectroscopy*, SIAM Journal on Imaging Sciences, (2009)

Piana et al., *Electron flux spectral imaging of solar flares through regularized analysis of hard x-ray source visibilities,* The Astrophysical Journal, (2007)

From count to electron visibilities

Count visibilities:

$$V(u,v;q) = \int_X \int_Y J(x,y;q) e^{2\pi\imath(xu+yv)}\, dx\, dy \tag{1}$$

Electron flux visibility spectrum:

$$W(u,v;E) = \int_X \int_Y \mathcal{F}(x,y;E) e^{2\pi\imath(xu+yv)}\, dx\, dy \tag{2}$$

Bremsstralhung equation for visibilities:

$$V(u,v;q) = \frac{1}{4\pi R^2} \int_q^\infty W(u,v;E) K(q,E)\, dE \tag{3}$$

Prato et al., *A Regularized Visibility-Based Approach to Astronomical Imaging Spectroscopy*, SIAM Journal on Imaging Sciences, (2009)

Piana et al., *Electron flux spectral imaging of solar flares through regularized analysis of hard x-ray source visibilities,* The Astrophysical Journal, (2007)

Visibility inversion algorithm

Count visibilities

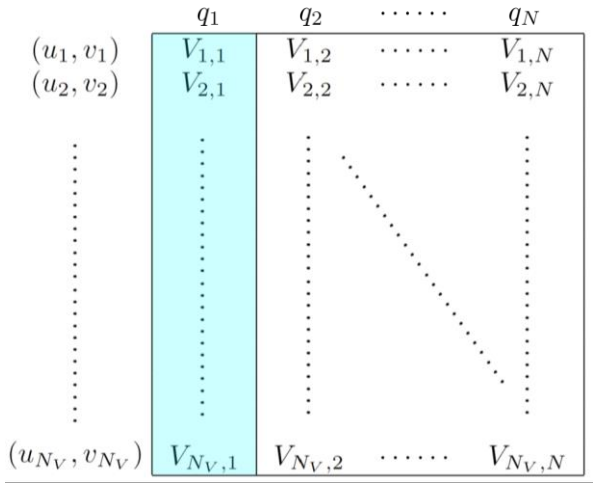

Prato et al., *A Regularized Visibility-Based Approach to Astronomical Imaging Spectroscopy*, SIAM Journal on Imaging Sciences, (2009)

Piana et al., *Electron flux spectral imaging of solar flares through regularized analysis of hard x-ray source visibilities,* The Astrophysical Journal, (2007)

Visibility inversion algorithm

Solving image reconstruction problem via imaging methods

Count visibilities

$$
\begin{array}{c|cccc}
 & q_1 & q_2 & \cdots\cdots & q_N \\
\hline
(u_1, v_1) & V_{1,1} & V_{1,2} & \cdots\cdots & V_{1,N} \\
(u_2, v_2) & V_{2,1} & V_{2,2} & \cdots\cdots & V_{2,N} \\
\vdots & \vdots & \vdots & \ddots & \vdots \\
(u_{N_V}, v_{N_V}) & V_{N_V,1} & V_{N_V,2} & \cdots\cdots & V_{N_V,N}
\end{array}
$$

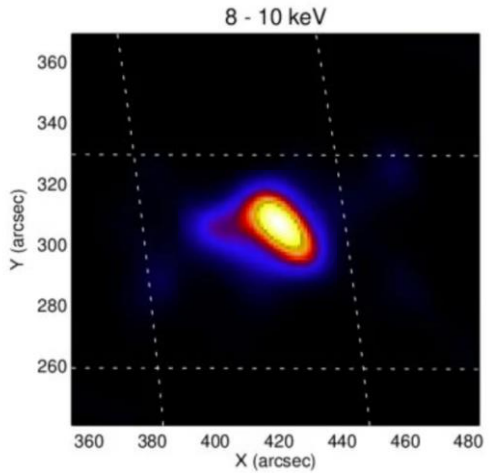

Figure: Reconstruction provided by MEM_GE, from count visibilities.

Prato et al., *A Regularized Visibility-Based Approach to Astronomical Imaging Spectroscopy*, SIAM Journal on Imaging Sciences, (2009)

Piana et al., *Electron flux spectral imaging of solar flares through regularized analysis of hard x-ray source visibilities,* The Astrophysical Journal, (2007)

Visibility inversion algorithm

Count visibilities

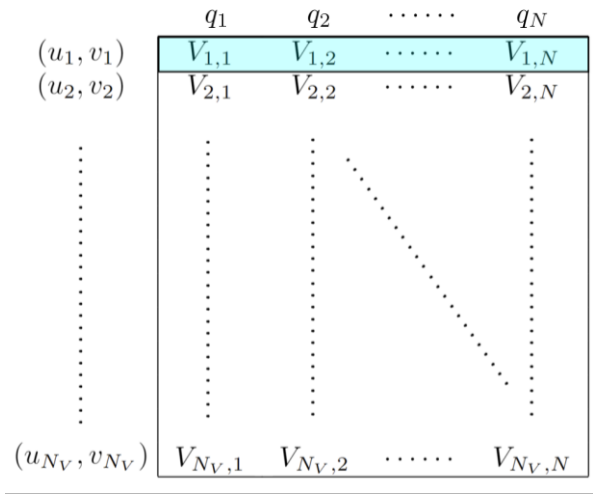

Prato et al., *A Regularized Visibility-Based Approach to Astronomical Imaging Spectroscopy*, SIAM Journal on Imaging Sciences, (2009)

Piana et al., *Electron flux spectral imaging of solar flares through regularized analysis of hard x-ray source visibilities,* The Astrophysical Journal, (2007)

Visibility inversion algorithm

Spectral inversion via regularized inversion technique (Tikhonov)

Count visibilities

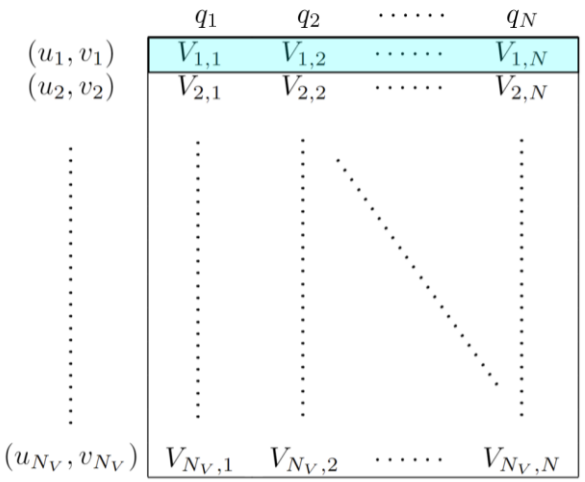

Electron visibilities

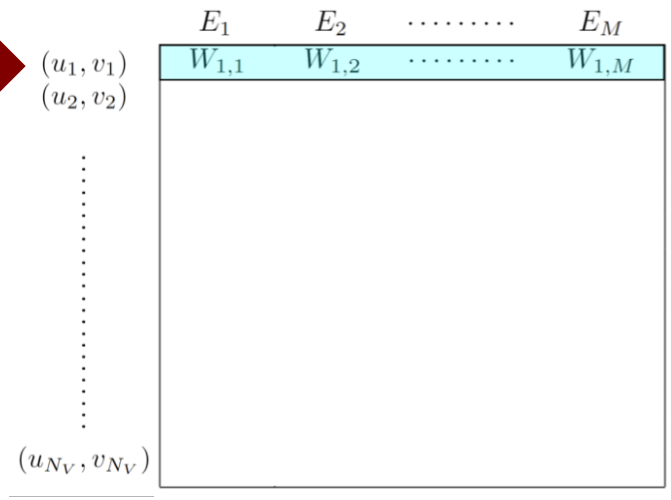

Prato et al., *A Regularized Visibility-Based Approach to Astronomical Imaging Spectroscopy*, SIAM Journal on Imaging Sciences, (2009)

Piana et al., *Electron flux spectral imaging of solar flares through regularized analysis of hard x-ray source visibilities,* The Astrophysical Journal, (2007)

Visibility inversion algorithm

Spectral inversion via regularized inversion technique (Tikhonov)

Count visibilities

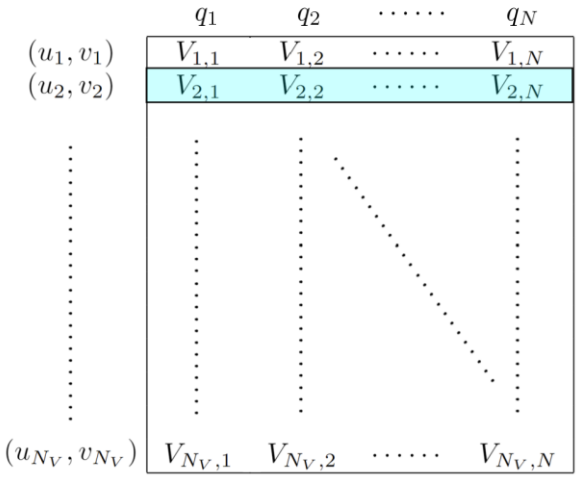

Electron visibilities

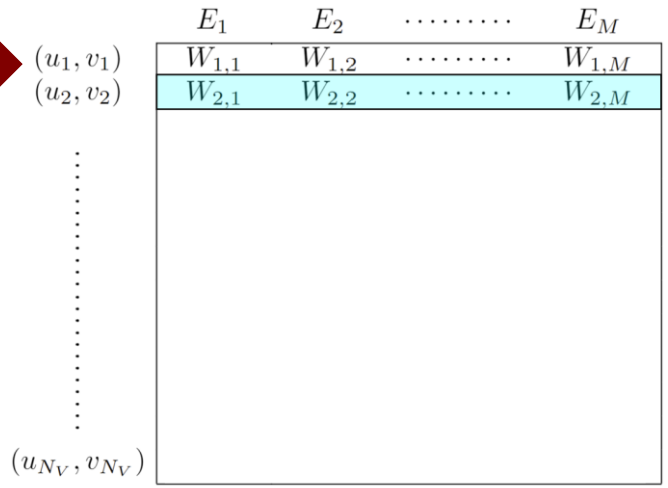

Prato et al., *A Regularized Visibility-Based Approach to Astronomical Imaging Spectroscopy*, SIAM Journal on Imaging Sciences, (2009)

Piana et al., *Electron flux spectral imaging of solar flares through regularized analysis of hard x-ray source visibilities,* The Astrophysical Journal, (2007)

Visibility inversion algorithm

Spectral inversion via regularized inversion technique (Tikhonov)

Count visibilities

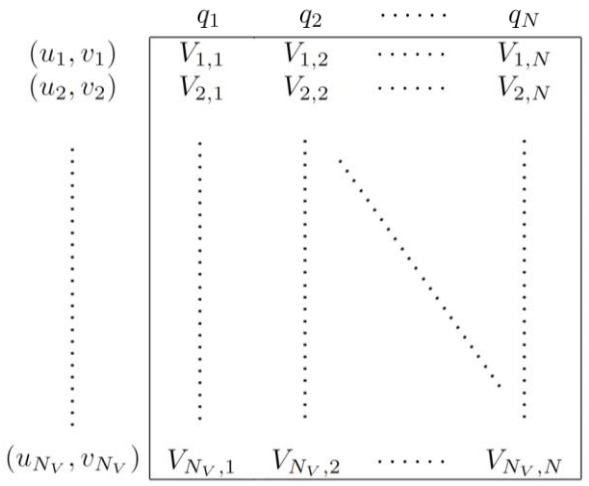

Electron visibilities

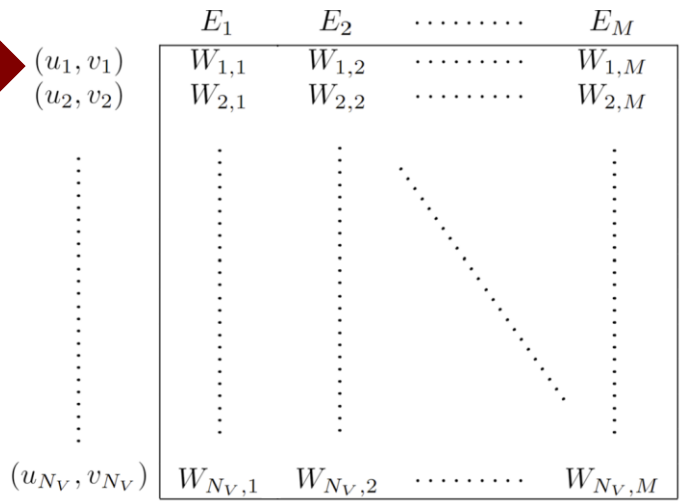

Prato et al., *A Regularized Visibility-Based Approach to Astronomical Imaging Spectroscopy*, SIAM Journal on Imaging Sciences, (2009)

Piana et al., *Electron flux spectral imaging of solar flares through regularized analysis of hard x-ray source visibilities,* The Astrophysical Journal, (2007)

Visibility inversion algorithm

Spectral inversion via regularized inversion technique (Tikhonov)

Solving image reconstruction problem via imaging methods.

Count visibilities

$$\begin{array}{c|cccc} & q_1 & q_2 & \cdots\cdots & q_N \\ (u_1, v_1) & V_{1,1} & V_{1,2} & \cdots\cdots & V_{1,N} \\ (u_2, v_2) & V_{2,1} & V_{2,2} & \cdots\cdots & V_{2,N} \\ \vdots & \vdots & \vdots & & \vdots \\ (u_{N_V}, v_{N_V}) & V_{N_V,1} & V_{N_V,2} & \cdots\cdots & V_{N_V,N} \end{array}$$

Electron visibilities

$$\begin{array}{c|cccc} & E_1 & E_2 & \cdots\cdots & E_M \\ (u_1, v_1) & W_{1,1} & W_{1,2} & \cdots\cdots & W_{1,M} \\ (u_2, v_2) & W_{2,1} & W_{2,2} & \cdots\cdots & W_{2,M} \\ \vdots & \vdots & \vdots & & \vdots \\ (u_{N_V}, v_{N_V}) & W_{N_V,1} & W_{N_V,2} & \cdots\cdots & W_{N_V,M} \end{array}$$

May 7, 2021 – 18:51 UT

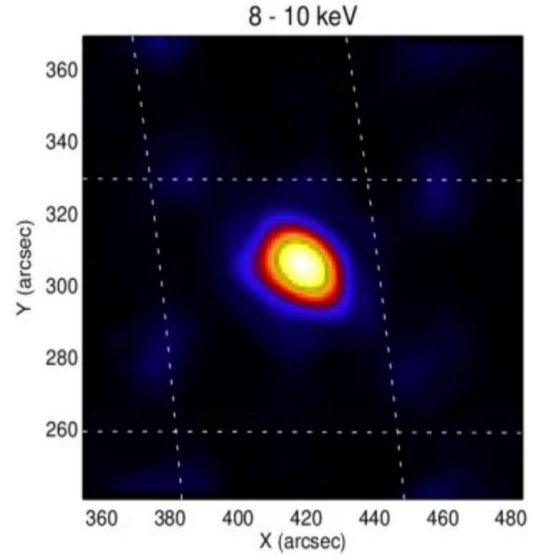

Figure: Reconstruction provided by MEM_GE, from electron visibilities.

Prato et al., *A Regularized Visibility-Based Approach to Astronomical Imaging Spectroscopy*, SIAM Journal on Imaging Sciences, (2009)

Piana et al., *Electron flux spectral imaging of solar flares through regularized analysis of hard x-ray source visibilities,* The Astrophysical Journal, (2007)

Outline

1. From count to electron visibilities & Visibility inversion algorithm
2. **Results**
3. Conclusions and future works

Results – September 29, 2022

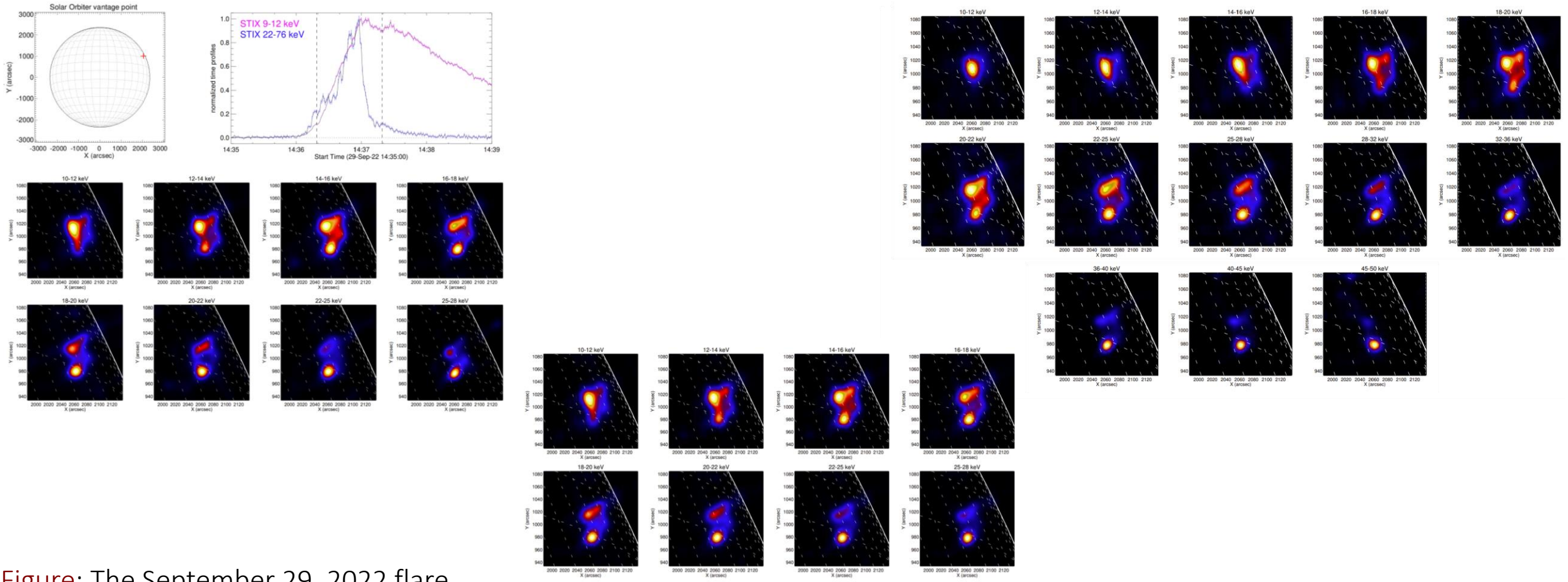

Figure: The September 29, 2022 flare.
Left panel, *top row*: position of the event on the solar disk and normalized STIX time profiles. *Bottom rows*: count images of the event at different energies. **Right panel**: electron flux images in different energy channels. **Middle panel**: Regularized count maps in different energy channels.

Results – September 29, 2022

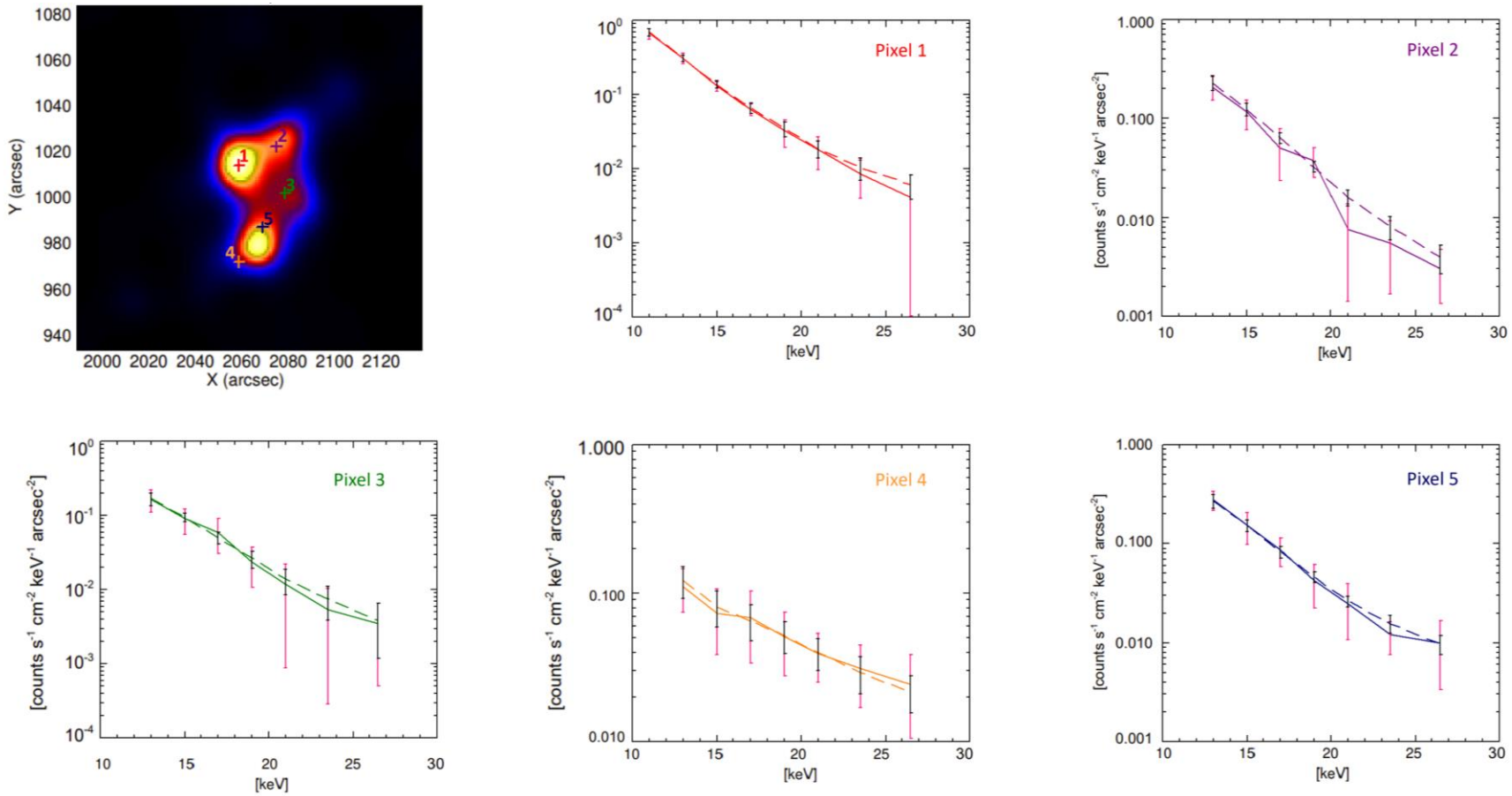

Figure: Spatially resolved count spectra. *Top left panel*: Selected pixels are indicated with colored crosses. Other panels show the corresponding pixel-wise spectra obtained from count images (solid line) and regularized count images (dashed line). The pixels selected in the top left panel and their respective spectra are indicated with the same color. The plots are logarithmically scaled on the y-axis. The (3σ)-error bars on the count spectra are in pink, while the error bars on the regularized count spectra are in black.

Results – May 08, 2021

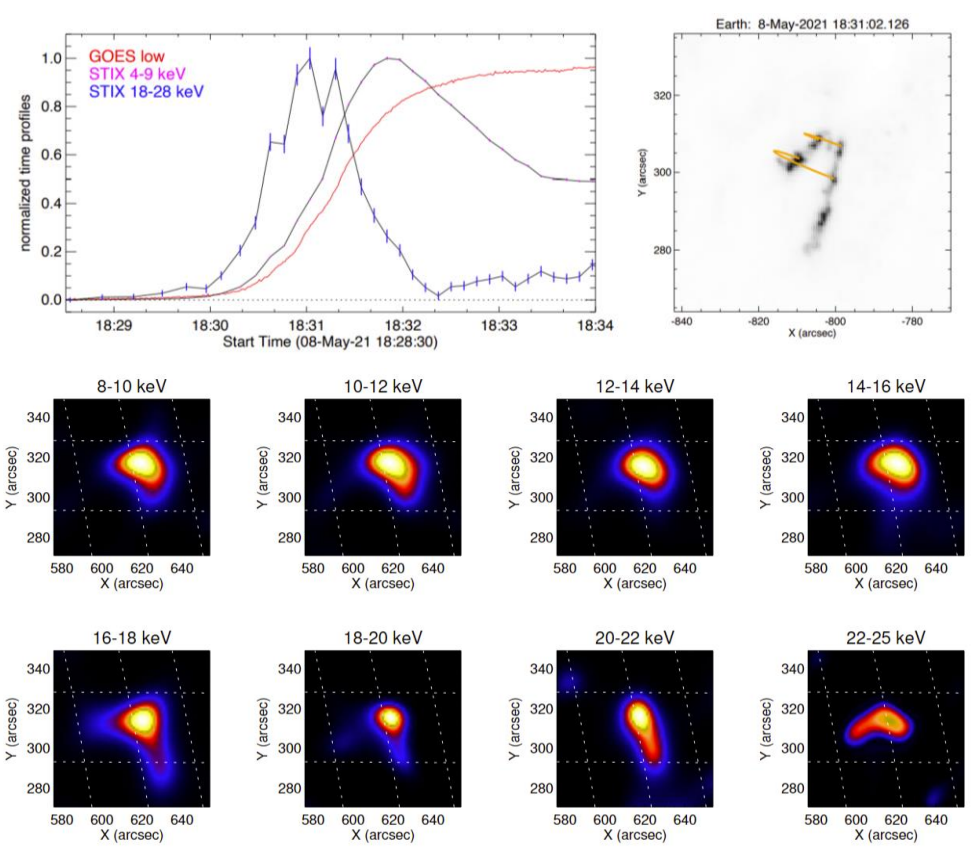

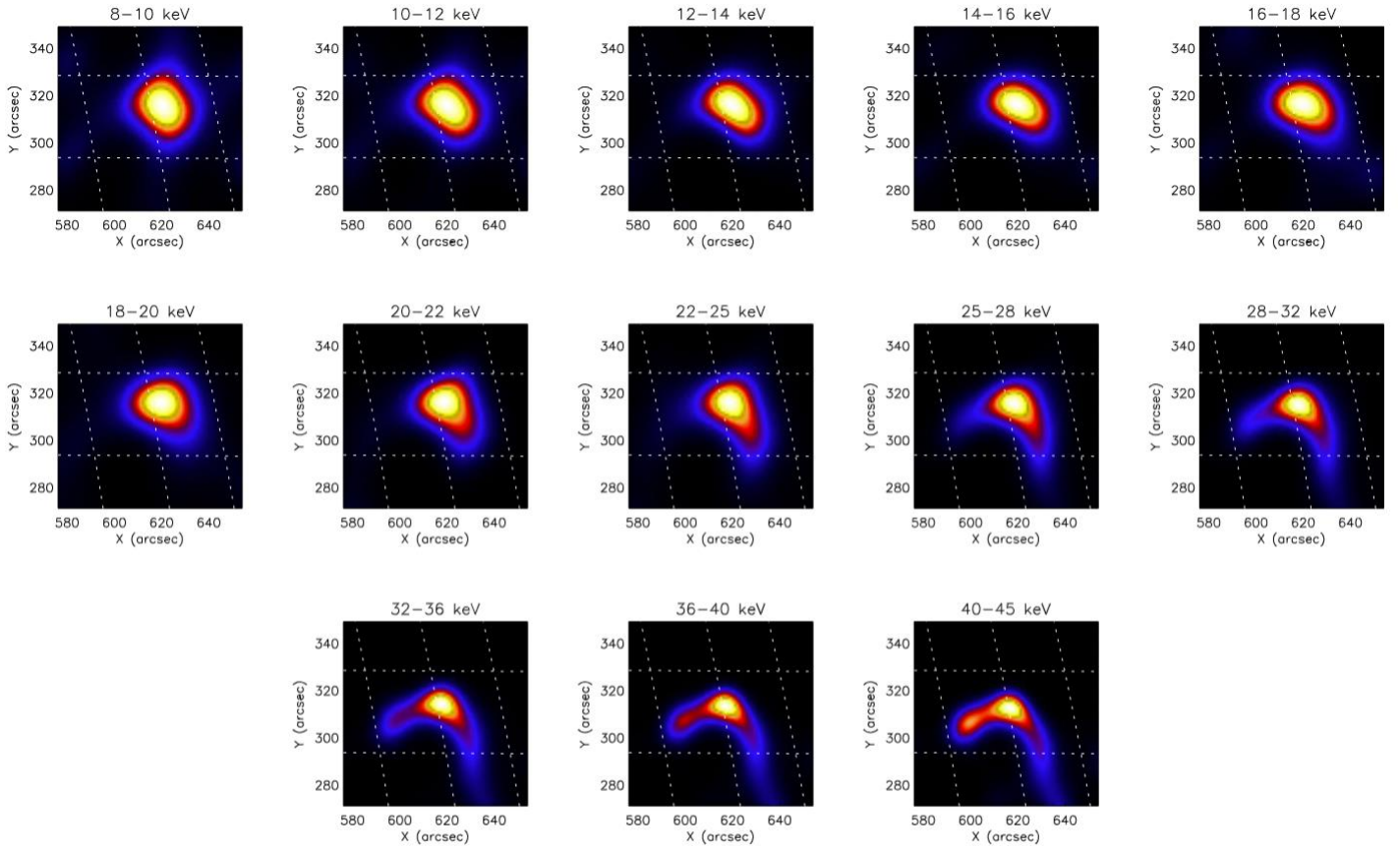

Figure: The May 08, 2021, flare.
Left panel, *top row*: normalized GOES and STIX time profiles, and AIA 1600 Å image. *Bottom rows*: count images of the event at different energies. **Right panel**: electron flux images in different energy channels.

Results – May 08, 2021

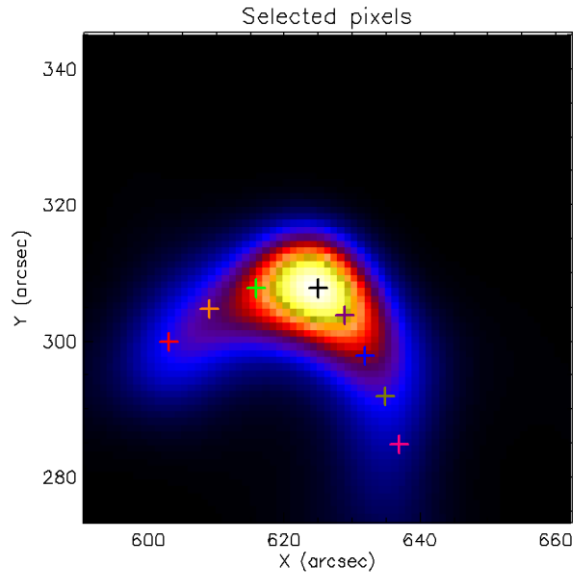

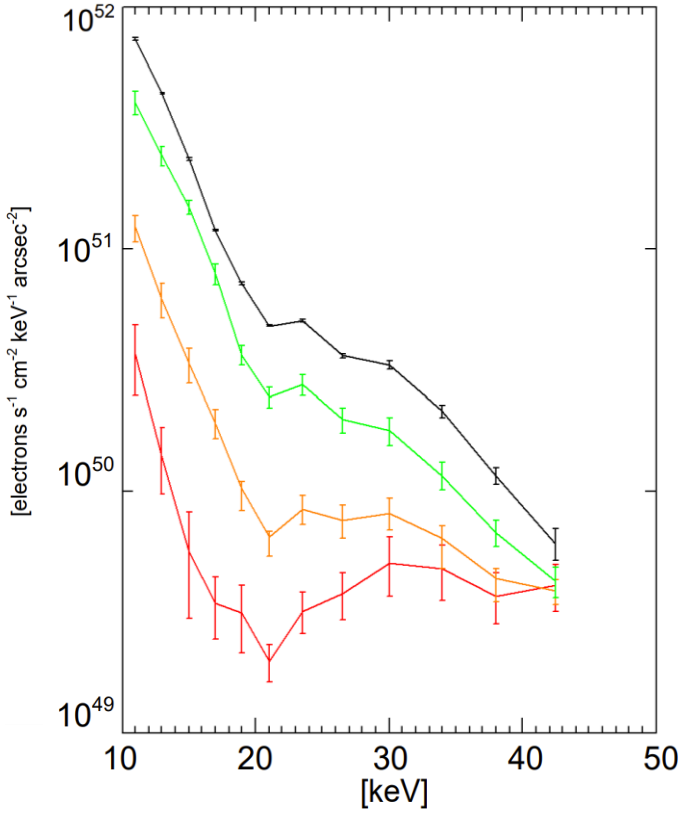

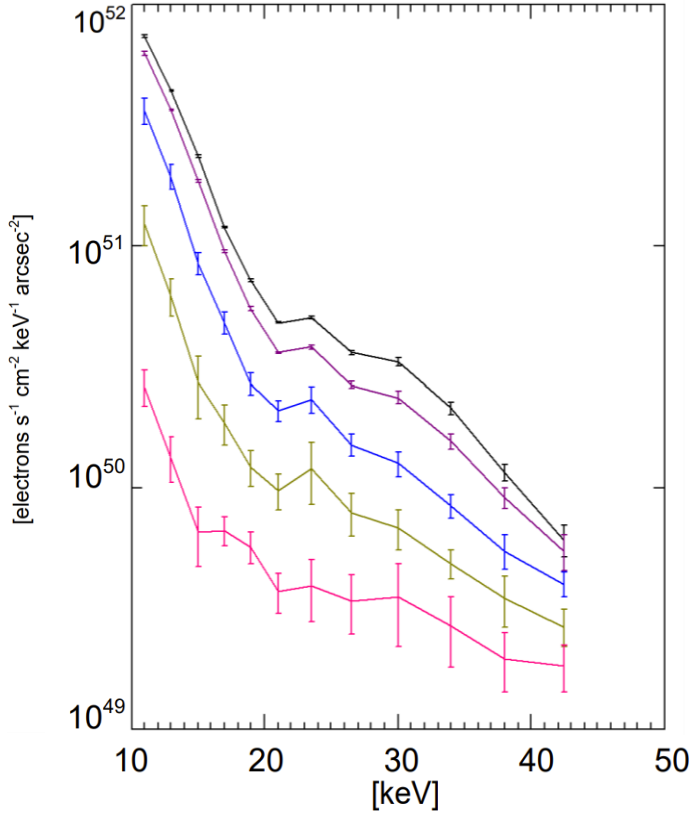

Figure: *Left panel*: electron flux map in the energy channel 28-32 keV, with seven locations identified in the loop *Middle and right panels*: regularized electron flux spectra at these seven locations, with 3σ uncertainties shown at each point. The spectra are obtained by considering areas of 5 × 5 arc seconds around each of the selected points and averaging the corresponding spectra. The spectra clearly show two components: a thermal component below ~20 keV and a non-thermal component at higher energies.

Results – Validation

Event	OSPEX	electron flux spectral images	count images	regularized count images
May 08, 2021	$\gamma = 5.28 \pm 0.18$	$\delta = 4.53 \pm 0.07$	$\gamma = 4.94 \pm 0.24$	$\gamma = 5.50 \pm 0.04$
August 26, 2021	$\gamma = 5.65 \pm 0.12$	$\delta = 4.59 \pm 0.11$	$\gamma = 5.27 \pm 0.17$	$\gamma = 5.57 \pm 0.06$
January 20, 2022	$\gamma = 6.51 \pm 0.26$	$\delta = 5.07 \pm 0.03$	$\gamma = 6.25 \pm 0.14$	$\gamma = 6.36 \pm 0.01$
August 28, 2022	$\gamma = 6.74 \pm 0.18$	$\delta = 4.97 \pm 0.04$	$\gamma = 6.88 \pm 0.24$	$\gamma = 6.81 \pm 0.03$
September 29, 2022	$\gamma = 4.54 \pm 0.05$	$\delta = 3.68 \pm 0.01$	$\gamma = 4.24 \pm 0.11$	$\gamma = 4.42 \pm 0.01$

Table: *First column*: event date. *Second column*: photon power-law index γ obtained by fitting spatially integrated spectra with OSPEX. *Third column*: electron power-law index δ obtained by fitting spatially integrated electron flux spectral images. *Fourth and fifth columns*: photon power-law index γ obtained by fitting spatially integrated count images and spatially integrated regularized count images, respectively, assuming a diagonal response of unity. The uncertainties in columns 3, 4, and 5 are determined by repeating the computation for 10 random realizations of the input visibilities.

Results – Validation

Event	OSPEX	electron flux spectral images	count images	regularized count images
May 08, 2021	$\gamma = 5.28 \pm 0.18$	$\delta = 4.53 \pm 0.07$	$\gamma = 4.94 \pm 0.24$	$\gamma = 5.50 \pm 0.04$
August 26, 2021	$\gamma = 5.65 \pm 0.12$	$\delta = 4.59 \pm 0.11$	$\gamma = 5.27 \pm 0.17$	$\gamma = 5.57 \pm 0.06$
January 20, 2022	$\gamma = 6.51 \pm 0.26$	$\delta = 5.07 \pm 0.03$	$\gamma = 6.25 \pm 0.14$	$\gamma = 6.36 \pm 0.01$
August 28, 2022	$\gamma = 6.74 \pm 0.18$	$\delta = 4.97 \pm 0.04$	$\gamma = 6.88 \pm 0.24$	$\gamma = 6.81 \pm 0.03$
September 29, 2022	$\gamma = 4.54 \pm 0.05$	$\delta = 3.68 \pm 0.01$	$\gamma = 4.24 \pm 0.11$	$\gamma = 4.42 \pm 0.01$

Table: *First column*: event date. *Second column*: photon power-law index γ obtained by fitting spatially integrated spectra with OSPEX. *Third column*: electron power-law index δ obtained by fitting spatially integrated electron flux spectral images. *Fourth and fifth columns*: photon power-law index γ obtained by fitting spatially integrated count images and spatially integrated regularized count images, respectively, assuming a diagonal response of unity. The uncertainties in columns 3, 4, and 5 are determined by repeating the computation for 10 random realizations of the input visibilities.

Results – Validation

Event	OSPEX	electron flux spectral images	count images	regularized count images
May 08, 2021	$\gamma = 5.28 \pm 0.18$	$\delta = 4.53 \pm 0.07$	$\gamma = 4.94 \pm 0.24$	$\gamma = 5.50 \pm 0.04$
August 26, 2021	$\gamma = 5.65 \pm 0.12$	$\delta = 4.59 \pm 0.11$	$\gamma = 5.27 \pm 0.17$	$\gamma = 5.57 \pm 0.06$
January 20, 2022	$\gamma = 6.51 \pm 0.26$	$\delta = 5.07 \pm 0.03$	$\gamma = 6.25 \pm 0.14$	$\gamma = 6.36 \pm 0.01$
August 28, 2022	$\gamma = 6.74 \pm 0.18$	$\delta = 4.97 \pm 0.04$	$\gamma = 6.88 \pm 0.24$	$\gamma = 6.81 \pm 0.03$
September 29, 2022	$\gamma = 4.54 \pm 0.05$	$\delta = 3.68 \pm 0.01$	$\gamma = 4.24 \pm 0.11$	$\gamma = 4.42 \pm 0.01$

Table: *First column*: event date. *Second column*: photon power-law index γ obtained by fitting spatially integrated spectra with OSPEX. *Third column*: electron power-law index δ obtained by fitting spatially integrated electron flux spectral images. *Fourth and fifth columns*: photon power-law index γ obtained by fitting spatially integrated count images and spatially integrated regularized count images, respectively, assuming a diagonal response of unity. The uncertainties in columns 3, 4, and 5 are determined by repeating the computation for 10 random realizations of the input visibilities.

Results – STIX vs. RHESSI

	STIX	**RHESSI**
Distance from the Sun	Variable	Fixed
Energy sampling	Non-uniform	Uniform
Gaps	provides its set of visibility values at all count energies → no (u, v) point gaps	gaps due to insufficient signal-to-noise as the visibility value in question → different energy bins have different number of samples

Table: Differences between STIX and RHESSI.

Results – STIX vs. RHESSI

Event	counts	electrons
September 29, 2022 (STIX)	0.061 ± 0.007	0.069 ± 0.019
February 20, 2002 (RHESSI)	0.114 ± 0.027	0.171 ± 0.067
January 11, 2023 (STIX)	0.058 ± 0.012	0.065 ± 0.035
December 02, 2003 (RHESSI)	0.124 ± 0.025	0.292 ± 0.225
November 11, 2022 (STIX)	0.070 ± 0.013	0.084 ± 0.032
February 20, 2002 (RHESSI)	0.128 ± 0.029	0.167 ± 0.038

Table: Analysis of CLEAN reconstructions for regularized counts and electron flux spectral images obtained using RHESSI and STIX visibilities. The *second and third columns* show the ratio of the residual and CLEANed maps peaks for the regularized count and electron flux spectral images, respectively, averaged across count and electron energies.

Outline

1. From count to electron visibilities & Visibility inversion algorithm
2. Results
3. **Conclusions and future works**

Conclusions and future works

- ☑ We have described an approach to solar hard X-ray imaging spectroscopy:
  - ☑ two-dimensional Fourier transforms of the image in the photon domain are transformed into Fourier transforms of the electron flux maps.
  - ☑ This tool also provides regularized photon visibilities corresponding to the regularized electron visibilities.

Conclusions and future works

- ☑ We have described an approach to solar hard X-ray imaging spectroscopy:
  - ☑ two-dimensional Fourier transforms of the image in the photon domain are transformed into Fourier transforms of the electron flux maps.
  - ☑ This tool also provides regularized photon visibilities corresponding to the regularized electron visibilities.

- ☑ Research products in the STIX framework have better quality than those obtained with RHESSI approach.

Conclusions and future works

- ☑ We have described an approach to solar hard X-ray imaging spectroscopy:
  - ☑ two-dimensional Fourier transforms of the image in the photon domain are transformed into Fourier transforms of the electron flux maps.
  - ☑ This tool also provides regularized photon visibilities corresponding to the regularized electron visibilities.
- ☑ Research products in the STIX framework have better quality than those obtained with RHESSI approach.
- ☑ We show how the spectrum of the accelerated electron flux varies from the corona to the chromospheric regions.

Conclusions and future works

- ☑ We have described an approach to solar hard X-ray imaging spectroscopy:
  - ☑ two-dimensional Fourier transforms of the image in the photon domain are transformed into Fourier transforms of the electron flux maps.
  - ☑ This tool also provides regularized photon visibilities corresponding to the regularized electron visibilities.
- ☑ Research products in the STIX framework have better quality than those obtained with RHESSI approach.
- ☑ We show how the spectrum of the accelerated electron flux varies from the corona to the chromospheric regions
- ❑ We are working to separate the mean electron flux and the ambient electron density factors.

References

- Brown et al., *Fast spectral fitting of hard X-ray bremsstrahlung from truncated power-law electron spectra*, Astronomy and Astrophysics, (2008)
- Koch & Motz, *Bremsstrahlung cross-section formulas and related data*, *Reviews of modern physics*, 1959, 31.4: 920
- Krucker et al., *The Spectrometer/Telescope for Imaging X-rays (STIX),* Astronomy and Astrophysics, (2020)
- Massa et al., *First Hard X-Ray Imaging Results by Solar Orbiter STIX*, Solar Physics, (2022)
- Massa et al., *MEM_GE: A New Maximum Entropy Method for Image Reconstruction from Solar X-Ray Visibilities*, The Astrophysical Journal, (2020)
- Massa et al*., The STIX Imaging Concept*, Solar Physics, 298, 114 (2023)
- Massone et al., *Regularized solution of the solar Bremsstrahlung inverse problem: model dependence and implementation issues*, Inverse Problems in Science and Engineering, (2004)
- Piana, *Inversion of bremsstrahlung spectra emitted by solar plasma. In: SVD and Signal Processing III*, Elsevier Science BV, p. 475-484 (1995)
- Piana et al., *Hard X-rays imaging of Solar Flares*, Springer, (2022)
- Piana et al., *Electron flux spectral imaging of solar flares through regularized analysis of hard x-ray source visibilities,* The Astrophysical Journal, (2007)
- Piana et al., *Regularized electron flux spectra in the 2002 July 23 solar flare,* The Astrophysical Journal, 595.2: L127, (2003)
- Prato et al., *A Regularized Visibility-Based Approach to Astronomical Imaging Spectroscopy*, SIAM Journal on Imaging Sciences, (2009)

THANK YOU FOR THE ATTENTION!

Università di Genova
DIMA | Dipartimento di Matematica
MIDA group